

Reduced-Rank STAP for Optimum Detection by Antenna-Pulse Selection

Xiangrong Wang, Elias Aboutanios, Moeness G. Amin

Abstract—Space-time adaptive processing (STAP) is an effective strategy for clutter suppression in airborne radar systems. Limited training data, high computational load and the heterogeneity of training data constitute the main challenges in STAP. Most reduced-rank detection approaches, such as eigenvector decomposition, utilise a linear transformation to reduce the problem dimensionality. In this letter, we propose a new detection strategy based on selecting an optimum subset of antenna-pulse pairs associated with maximum separation between the target and the clutter trajectory. The proposed strategy reduces redundancy while addressing the above three interlinked challenges. An iterative Min-Max algorithm is proposed to solve the antenna-pulse selection problem, which is NP-hard combinatorial optimization. Extensive simulation results confirm the effectiveness of the proposed strategy.

Index Terms—STAP, Heterogeneous clutter, Clutter trajectory, Combinatorial optimization, Min-Max algorithm

I. INTRODUCTION

Space-time adaptive processing (STAP) is a well-established framework for the detection of slow-moving targets in airborne radar systems with strong clutter interference, see [1], [2], [3], [4] and the references therein. The optimum STAP processor employs the clutter-plus-noise covariance matrix (CCM) to whiten the received data prior to the application of a matched-filter detector. In practical applications, the true CCM is not available and is usually estimated from secondary range cells, using for example the sample matrix inversion (SMI) method. The number of independent and identically distributed (IID) training data, required by the SMI to ensure an average signal-to-clutter-plus-noise ratio (SCNR) loss within 3dB of the optimum processor, is twice the number of degrees of freedom (DoFs) of the detector. This is usually on the order of several hundreds for typical STAP applications [5] and can far exceed the available data measurements [6]. In a homogeneous environment, where the secondary range gates share the same CCM with the cell under test (CUT), the SMI maximizes the SCNR [7]. However, when the environment is non-homogeneous, the SMI may incur a significant performance degradation [8].

In real-world scenarios, practical implementations of STAP continue to face a number of challenges including limited sample support, clutter heterogeneity, and computational cost. These problems have been studied extensively in the literature

and solutions have been proposed to address each of them. For instance, preprocessing can be used to select statistically representative training data in order to mitigate clutter heterogeneity, [9], [10], [11]. Knowledge-aided (KA) STAP incorporates *a priori* knowledge into the estimation process to accelerate the convergence of the CCM, [12], [13]. Test data only algorithms such as the D^3 algorithm, [14], and the MLD, [15], do away with the need for training data. An image processing-based STAP technique was proposed in [16]. Alternatively, the problem dimensionality can be reduced by projecting the data onto a lower dimensional subspace, which reduces the sample support requirement. Principle Component Analysis (PCA) constructs the projection matrix from the eigenvectors of the CCM [17], [18]. Other transformation methods can be found in [19], [20] and references therein.

In addition to clutter heterogeneity, the computational cost of the full optimum processor is also problematic. A radar array with N antennas and M coherent pulses involves the inversion of an $NM \times NM$ matrix, requiring an order of $(NM)^3$ operations. The fact that the algorithm must be executed for each range gate, as well as angle and Doppler bins exacerbates the problem. Traditional projection methods, like PCA, reduce the high sample support by determining the projection matrix adaptively, but do not alleviate the computational load. Among all available strategies, reducing the DoFs prior to the processing is most desirable as it simultaneously tackles the three aforementioned problems [21]. Specifically, it leads to a lower computational load, fewer training data required, and improved robustness to clutter heterogeneity. In this paper, we propose a novel approach consisting of an antenna-pulse selection strategy where we choose the optimal $K < MN$ antenna-pulse pairs in each range gate before STAP and detection. The goal is to select the antenna-pulse pairs that give significantly better performance compared to the standard, consecutively sampled, antenna-pulse pairs. The selection is carried out such that the resulting space-time configuration attenuates clutter returns while maximising the target response. In [22], Ward examined the application of thinned arrays in airborne radar to reject ground clutter. It was shown that the effective rank of the CCM depends on the precise thinned array configuration [22]. However, the selection of the optimum subarray was not discussed, and the thinned array which preserves the clutter rank may not lead to the best performance. Unlike [22], we carry out thinning in both space and time through joint antenna-pulse selection.

The paper is organized as follows: In section II, we review the clutter model, introduce the Space-Spectral Correlation Coefficient (S^2C^2), and propose an iterative Min-Max algorithm

X. Wang, E. Aboutanios are with the School of Electrical Engineering and Telecommunication, University of New South Wales, Sydney, Australia 2052. e-mail: x.r.wang@unsw.edu.au; elias@unsw.edu.au.

M. G. Amin is with the Center for Advanced Communications, College of Engineering, Villanova University, Villanova, PA 19085, USA. e-mail: moeness.amin@villanova.edu.

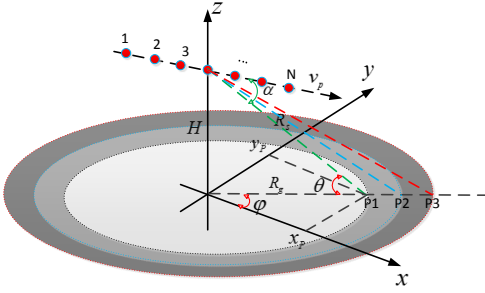


Fig. 1. Airborne radar geometry. The linear array is configured as sidelooking and moving along the x -direction. P_1 , P_2 and P_3 denote three adjacent range gates respectively.

to select the optimum space-time configuration. Section III gives simulation results that validate the performance of the proposed strategy for combatting the clutter heterogeneity and reducing the computational cost. Finally, some conclusions are drawn in section IV.

II. ANTENNA-PULSE SELECTION FOR CLUTTER SUPPRESSION

Consider a sidelooking radar having a uniform linear array (ULA) with N isotropic antennas as shown in Fig. 1. The radar transmits M coherent pulses with a pulse repetition interval (PRI) T . Without loss of generality, we assume the radar is moving along the positive x -direction with a velocity v_p .

A. Clutter Model

The phase difference between the returns corresponding to P_1 at two sensors separated by d is,

$$\Delta\varphi = 2\pi f_s = 2\pi \frac{d \cos \phi \cos \theta}{\lambda}, \quad (1)$$

where ϕ and θ are the azimuth and elevation angles respectively. f_s is the normalized spatial frequency and λ is the wavelength. The normalized clutter Doppler shift is given by

$$f_d = \frac{2v_p T}{\lambda} \cos \phi \cos \theta. \quad (2)$$

Thus, the length NM interleaved space-time steering vector of the clutter patch P_1 , $\mathbf{c}(f_s, f_d)$ comprises of the elements

$$c_{nm}(f_s, f_d) = e^{j2\pi(nf_s + mf_d)}, \quad (3)$$

for $n = 0, \dots, N-1$ and $m = 0, \dots, M-1$. The target space-time steering vector $\mathbf{s} \in \mathcal{C}^{NM \times 1}$ can be similarly derived.

Eqs. (1) and (2) reveal that, for a sidelooking radar, the trajectory of the clutter spectrum in the Spatial-Doppler plane is a straight line with slope $\beta = 2v_p T/d$. This implies that most of the clutter energy is concentrated in a ridge and the effective clutter rank is much smaller than NM . In fact, for a sidelooking ULA, Brennan's rule gives the effective rank of the CCM to be, [7],

$$N_r = \text{int}\{N + \beta(M - 1)\}, \quad (4)$$

where $\text{int}\{\}$ denotes the next integer number. This rule states that there are at most N_r clutter eigenvalues that are larger than the noise floor σ_n^2 . In other words, the clutter subspace is

spanned by the N_r eigenvectors corresponding to the dominant eigenvalues. The remaining $NM - N_r$ eigenvectors span the white noise subspace. Note that the signal space is also spanned by the Angle-Doppler steering vectors and there exists a unitary transformation between the Eigenvector and Fourier basis vectors. This unitary transformation "spreads" the clutter energy over a larger subset of Fourier basis vectors. However, as shown in [23], for large enough clutter-to-noise ratio (CNR), the clutter trajectory is well defined by Fourier basis vectors, and the number of clutter eigenvalues corresponds to the number of Angle-Doppler cells where the clutter power is significant. Thus, the center points of the resolution grids along the clutter trajectory can be used as a set of approximate Fourier basis vectors of the clutter subspace, which circumvents the need for the computationally expensive eigenvalue decomposition. Clearly there is no specific rule that governs this choice and the simplest approach is to choose the cells where the clutter power is largest. Better clutter representation and performance is achieved by including more Fourier basis vectors at the expense of increased complexity. Thus, using Eq. (3), the approximate set of Fourier basis of the clutter subspace is given by $[\mathbf{c}(f_s^1, f_d^1), \mathbf{c}(f_s^2, f_d^2), \dots, \mathbf{c}(f_s^{N_r}, f_d^{N_r})]$.

B. Spatial Spectral Correlation Coefficient

Let $\mathbf{c}(f_s, f_d)$ be a clutter steering vector corresponding to the frequency (f_s, f_d) . We define the S^2C^2 as

$$\alpha = \frac{\mathbf{s}^H \mathbf{c}(f_s, f_d)}{\sqrt{(\mathbf{s}^H \mathbf{s})(\mathbf{c}(f_s, f_d)^H \mathbf{c}(f_s, f_d))}} = \frac{\mathbf{s}^H \mathbf{c}(f_s, f_d)}{NM}. \quad (5)$$

This definition extends the Spatial Correlation Coefficient (SCC) of [24] to a two-dimensional parameter. Similarly to the SCC, $|\alpha| \in [0, 1]$ and the S^2C^2 represents the angle between the target and clutter steering vectors. The smaller the value of the S^2C^2 is, the more separable the target and clutter are, thereby implying better adaptive processing performance. The motivation of this work is to reduce the number of antennas and pulses, thereby reducing the number of DoFs, while enhancing performance by minimizing the S^2C^2 .

C. Iterative Min-Max Algorithm

The antenna-pulse selection strategy aims to maximize the SCNR for the expected worst case clutter covariance, [25]. To this end, we propose a Min-Max algorithm that minimises the maximum S^2C^2 between the target steering vector and the selected N_r clutter steering vectors. Let us define a selection vector $\mathbf{z} \in \{0, 1\}^{NM}$, where an entry of one implies that the corresponding antenna-pulse pair is selected, and zero means it is discarded. Then, the problem is formulated as

$$\begin{aligned} \min_{\mathbf{z}, t} \quad & t, \\ \text{s.t.} \quad & \mathbf{z}^T \mathbf{W}_{cs}^i \mathbf{z} \leq t, i = 1, \dots, N_r \\ & \mathbf{z} \in \{0, 1\}^{NM}, \\ & \mathbf{1}^T \mathbf{z} = K, \\ & t > 0. \end{aligned} \quad (6)$$

Here the correlation steering matrix is $\mathbf{W}_{cs}^i = \mathbf{w}_{cs} \mathbf{w}_{cs}^H$, and $\mathbf{w}_{cs} = \mathbf{c}^*(f_s^i, f_d^i) \odot \mathbf{s}$. \odot denotes the element-wise product

and \bullet^* is the conjugate of \bullet . K is the number of selected antenna-pulse pairs and $\mathbf{1}$ is the vector of ones.

In order to assess our strategy, we adopt the Adaptive Matched Filter (AMF) detector in this work [26]. The theoretical false alarm rate P_{FA} of the AMF for a standard ULA with K antenna-pulse pairs and K_t training data, is

$$P_{FA} = \int_0^1 \left(1 + \frac{\gamma\eta}{K_t}\right)^{-L} f_\beta(\eta; L+1, K-1) d\eta, \quad (7)$$

where γ is the threshold value of the AMF detector and $L = K_t - K + 1$. η is a type I beta distributed variable with parameters $L+1$ and $K-1$. The detection probability P_D , on the other hand, is

$$P_D = 1 - \int_0^1 h(\eta) f_\beta(\eta; L+1, K-1) d\eta, \quad (8)$$

where

$$h(\eta) = \left(1 + \frac{\gamma\eta}{K_t}\right)^{-L} \sum_{l=1}^L \binom{L}{l} \left(\frac{\gamma\eta}{K_t}\right)^l G_l\left(\frac{\eta K \rho}{1 + \frac{\gamma\eta}{K_t}}\right), \quad (9)$$

and

$$G_l(y) = e^{-y} \sum_{n=0}^l \frac{y^n}{n!}, \quad (10)$$

where ρ is the signal to noise ratio (SNR). The number K of selected antenna-pulse pairs can be determined from Eq. (8) by setting P_{FA} , P_D and SNR to the desired values for actual scenarios. If only antenna selection is required for wide-band signal cases, this is a special case of Eq. (6). The problem of separately enforcing a number of selected antennas and pulses is more complicated and beyond the scope of this paper.

The optimization problem in Eq. (6) is convex except for the binary constraint $\mathbf{z} \in \{0, 1\}^{NM}$ which renders it an NP-hard combinatorial problem. To overcome this difficulty, we use the difference of convex sets (DCS) method, [24], to reformulate the optimization as

$$\begin{aligned} \min_{\mathbf{z}, t} \quad & t + \mu(\mathbf{1}^T \mathbf{z} - \mathbf{z}^T \mathbf{z}), \\ \text{s.t.} \quad & \mathbf{z} \mathbf{W}_{cs}^i \leq t, i = 1, \dots, N_r \\ & \mathbf{z} \in [0, 1]^{NM}, \\ & \mathbf{1}^T \mathbf{z} = K, \\ & t > 0, \end{aligned} \quad (11)$$

where μ is a regularization parameter that balances between the solution sparsity and S^2C^2 minimization. Finally, a sequential convex programming based on the first order Taylor decomposition is adopted to solve Eq. (11) iteratively. The k_{th} iteration of the Min-Max algorithm then becomes,

$$\begin{aligned} \min_{\mathbf{z}, t} \quad & t + \mu(\mathbf{1} - 2\mathbf{z}_{k-1})^T \mathbf{z}; \\ \text{s.t.} \quad & \mathbf{z} \mathbf{W}_{cs}^i \leq t, \quad i = 1, \dots, N_r \\ & \mathbf{z} \in [0, 1]^{NM}, \\ & \mathbf{1}^T \mathbf{z} = K, \\ & t > 0. \end{aligned} \quad (12)$$

It should be noted that Eqs. (6) and (11) are equivalent and have the same minimum objective value for large enough μ .

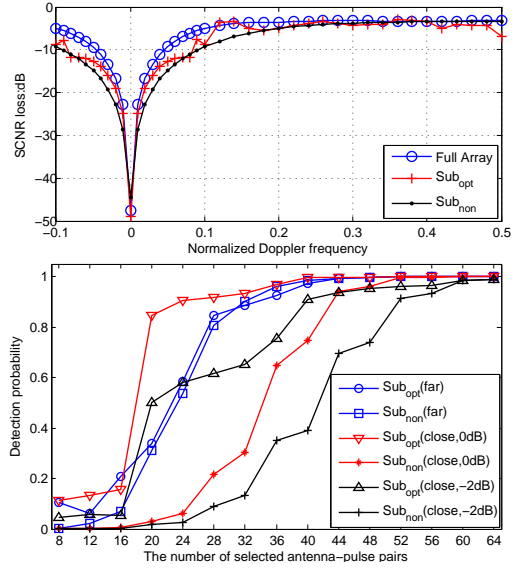


Fig. 2. (a) SCNR loss versus normalised Doppler frequency; (b) detection probability versus different numbers of selected antenna-pulse pairs (for $P_{FA} = 10^{-3}$). Each point is averaged over 10^5 Monte-Carlo runs.

III. SIMULATION RESULTS

In this section, we present simulation results to validate the effectiveness of the proposed strategy. We use an 8-antenna side-looking linear array transmitting a train of 8 coherent pulses satisfying the Displaced Phase Center Antenna (DPCA) condition. The number of IID training data required by the SMI algorithm to achieve an SCNR loss within 3 dB of the optimum is $2NM = 128$. However, as the effective rank of the clutter is 15 [2], we set the number of selected antenna-pulse pairs to $K = 16$, meaning that only $2K = 32$ training data snapshots are required. In all simulations, we assume the target is in broadside, that is it has an azimuth of 90° .

The performance of clutter suppression strategies in STAP is commonly assessed using the SCNR loss, [27],

$$L_s = \frac{\text{SCNR}_{\text{hete}}}{\text{SNR}} = \frac{(\mathbf{s}^H \hat{\mathbf{R}}_n^{-1} \mathbf{s})^2}{(\mathbf{s}^H \hat{\mathbf{R}}_n^{-1} \mathbf{R}_n \hat{\mathbf{R}}_n^{-1} \mathbf{s})(\mathbf{s}^H \mathbf{s} / \sigma_n^2)}, \quad (13)$$

where $\hat{\mathbf{R}}_n$ and \mathbf{R}_n are the estimated and true CCMs respectively and σ_n^2 is the white noise power. L_s compares the interference-limited performance to the noise-only case for each configuration. The simulation results are shown in Fig. 2(a). The target Doppler frequency sweeps over the range $[-0.1, 0.5]$ and we calculate the optimum set of antenna-pulse pairs corresponding to each frequency. We compare the optimum configuration, which we denote by sub_{opt} , to the non-optimum configuration, sub_{non} , consisting of the 16 samples obtained from the first 4 antennas and 4 pulses. The performance of the full configuration is also included for reference. Notice the significant gain in SCNR of the optimum sub-configuration with respect to sub_{non} when the target is close to the clutter ridge. Although both sub-configurations incur a SCNR loss with respect to the full configuration, the optimum sub-configuration, which maximises the separation between the target and clutter, recovers a large part of this loss

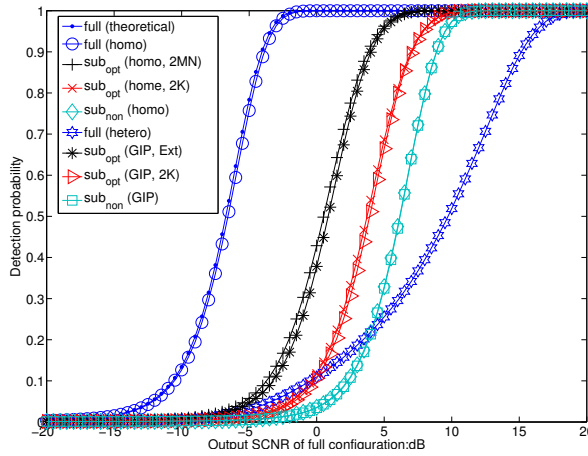


Fig. 3. Detection probability curve versus SCNR in both homogeneous and heterogeneous clutter, the target is close to the clutter trajectory, each point is averaged over 10^5 Monte-Carlo runs (for $P_{FA} = 10^{-3}$).

and gets closer to the full configuration performance. When the target is far from the clutter, all sub-configurations exhibit similar performance and there is no advantage to the proposed antenna-pulse selection strategy. Thus, the selection strategy is most useful for slow moving targets that are close to the clutter ridge.

Next we examine the relationship between the probability of detection and the number of selected antenna-pulse pairs K . The results, shown in Fig. 2(b), include two scenarios; one where the target is close to the clutter ridge, having Doppler frequency $f_d = 0.02$, and another where the target is far from the clutter with $f_d = 0.2$. For the close target, we show curves for SCNR values of both 0dB and -2dB. For each K , the optimum configuration is calculated and the non-optimum one is simply consisting of the first K consecutive antenna-pulse pairs. The results demonstrate the significant performance gain that the selection strategy achieves. When the target is far from the clutter, the non-optimum and optimum sub-configurations exhibit very similar performance and practically coincide. However, when the target is close to the clutter ridge, the performance of the non-optimum configuration degrades markedly, whereas that of the optimal sub-configuration does not. Importantly, we see that the optimum sub-configuration achieves the same detection performance as the full one for a much smaller number of DoFs. For instance, when the SCNR is 0dB, sub_{opt} needs only about 40 antenna-pulse pairs, whereas sub_{non} compared with 52 for the non-optimum sub-configuration.

Finally we illustrate the improvement in the detection probability that the selection strategy gives in both homogeneous and heterogeneous scenarios. In the simulation, the probability of false alarm rate is set to $P_{FA} = 10^{-3}$. As we are primarily interested in low-velocity targets, we assume the normalised target Doppler frequency to be uniformly distributed over the range $[0.005, 0.09]$. The simulation results are shown in Fig. 3. The labels “homo” and “hetero” refer to the homogeneous and heterogeneous environments respectively. In the homogeneous case, we obtain the detection curves for sub_{opt} when the CCM is estimated from 32 and 128 training data snapshots

respectively. Additionally, for reference, the theoretical P_d curve is plotted for the full configuration. In the heterogeneous scenario, we simulate the clutter heterogeneity by inserting 15 high-amplitude, mainbeam discrete targets into various range cells and Doppler frequencies [9]. The required training data snapshots for both sub-configurations are selected using the GIP-based non-homogeneity detector (NHD) of [9]. Specifically, we sort the GIP values and retain the $2K = 32$ realizations corresponding to smallest GIP value. Moreover, the curve labelled “Ext” is the result of using the maximum number of homogeneous snapshots that returned by the NHD. Note that the sub_{non} is the same as that used to obtain the SCNR loss results of Fig. 2(a). We make the following observations:

- The simulated and theoretical detection curves of the full configuration coincide in the homogeneous case;
- The optimum sub-configuration exhibits better performance than the non-optimum sub-configuration in both homogeneous and heterogeneous clutter;
- In heterogeneous clutter, both sub-configurations combined with the NHD outperform the full array. In fact they retain practically the same performance as the homogeneous case. Importantly, we see that the optimum sub-configuration shows the best detection performance.
- A deeper examination of the optimum sub-configuration reveals that it always maintains an effective clutter rank equal to that of the full configuration (that is 15). This allows for better clutter rejection, which is compared to a clutter rank of 9 for the non-optimal sub-configuration which may result in poor clutter suppression;
- When the target is close to the clutter trajectory, the optimum space-time configuration usually includes the extreme antenna-pulse pairs, thus preserving the maximum spatial-temporal aperture length.

IV. CONCLUSION

This paper proposed and investigated a novel antenna-pulse selection problem in order to enhance target detection performance of STAP while reducing the training data requirement, computational load and sensitivity to clutter heterogeneity. We proposed to use Spatial and Spectral Correlation Coefficient (S^2C^2) to characterise the space-time separation between the target and clutter steering vectors. We formulated the antenna-pulse selection problem as a minimisation of the S^2C^2 and presented an iterative Min-Max algorithm to select the optimum antenna pulse pairs for any particular scenario. The performance of the proposed antenna-pulse selection strategy was validated using simulations, which demonstrated its effectiveness at preserving the performance while reducing the computational load and addressing the problems of clutter heterogeneity and limited sample support.

ACKNOWLEDGMENT

The authors would like to thank Dr. Yimin Zhang with the Center for Advanced Communications, Villanova University, USA to give helpful suggestions for improving the paper’s quality.

REFERENCES

- [1] D. Fuhrmann, "Application of Toeplitz covariance estimation to adaptive beamforming and detection," *Signal Processing, IEEE Transactions on*, vol. 39, pp. 2194–2198, Oct 1991.
- [2] R. Klemm, *Principles of space-time adaptive processing*. The Institution of Electrical Engineers, 2002.
- [3] S. Kraut and L. Scharf, "The CFAR adaptive subspace detector is a scale-invariant GLRT," *Signal Processing, IEEE Transactions on*, vol. 47, pp. 2538–2541, Sep 1999.
- [4] M. Steiner and K. Gerlach, "Fast converging adaptive processor or a structured covariance matrix," *Aerospace and Electronic Systems, IEEE Transactions on*, vol. 36, pp. 1115–1126, Oct 2000.
- [5] J. Guerci, J. Goldstein, and I. Reed, "Optimal and adaptive reduced-rank STAP," *IEEE Transactions on Aerospace and Electronic Systems*, vol. 36, no. 2, pp. 647–663, 2000.
- [6] E. Aboutanios and B. Mulgrew, "Evaluation of the single and two data set STAP detection algorithms using measured data," in *Proc. IEEE International Geoscience and Remote Sensing Symposium IGARSS 2007*, pp. 494–498, 2007.
- [7] L. Brennan and L. Reed, "Theory of adaptive radar," *IEEE Transactions on Aerospace and Electronic Systems*, no. 2, pp. 237–252, 1973.
- [8] C. Richmond, "Performance of a class of adaptive detection algorithms in nonhomogeneous environments," *Signal Processing, IEEE Transactions on*, vol. 48, pp. 1248–1262, May 2000.
- [9] M. Rangaswamy, J. H. Michels, and B. Himed, "Statistical analysis of the non-homogeneity detector for STAP applications," *Digital Signal Processing*, vol. 14, no. 3, pp. 253–267, 2004.
- [10] E. Aboutanios and B. Mulgrew, "Heterogeneity detection for hybrid STAP algorithm," *IEEE Radar Conference, 2008*, pp. 1–4, May 2008.
- [11] D. J. Rabideau and A. Steinhardt, "Improved adaptive clutter cancellation through data-adaptive training," *Aerospace and Electronic Systems, IEEE Transactions on*, vol. 35, pp. 879–891, Jul 1999.
- [12] W. Melvin and J. Guerci, "Knowledge-aided signal processing: a new paradigm for radar and other advanced sensors," *IEEE Transactions on Aerospace and Electronic Systems*, vol. 42, pp. 983–996, July 2006.
- [13] S. Bidon, O. Besson, and J.-Y. Tourneret, "Knowledge-aided STAP in heterogeneous clutter using a hierarchical Bayesian algorithm," *IEEE Transactions on Aerospace and Electronic Systems*, vol. 47, pp. 1863–1879, July 2011.
- [14] T. Sarkar, H. Wang, S. Park, R. Adve, J. Koh, K. Kim, Y. Zhang, M. Wucjs, and R. Brown, "A Deterministic Least-Squares Approach to Space-Time Adaptive Processing (STAP)," *IEEE Transactions on Antennas and Propagation*, vol. 49, pp. 91–103, Jan. 2001.
- [15] E. Aboutanios and B. Mulgrew, "A STAP algorithm for radar target detection in heterogeneous environments," in *Proc. IEEE/SP 13th Workshop on Statistical Signal Processing*, pp. 966–971, 2005.
- [16] H. Deng, B. Himed, and M. Wicks, "Image feature-based space-time processing for ground moving target detection," *Signal Processing Letters, IEEE*, vol. 13, pp. 216–219, April 2006.
- [17] A. Haimovich and Y. Bar-Ness, "An eigenanalysis interference canceler," *Signal Processing, IEEE Transactions on*, vol. 39, no. 1, pp. 76–84, 1991.
- [18] C. H. Gierull, "Statistical analysis of the eigenvector projection method for adaptive spatial filtering of interference," *Radar, Sonar and Navigation, IEE Proceedings*, vol. 144, pp. 57–63, Apr 1997.
- [19] A. Shackelford, K. Gerlach, and S. Blunt, "Partially Adaptive STAP using the FRACTA Algorithm," *IEEE Transactions on Aerospace and Electronic Systems*, vol. 45, pp. 58–69, Jan 2009.
- [20] R. Fa, R. De Lamare, and L. Wang, "Reduced-rank STAP schemes for airborne radar based on switched joint interpolation, decimation and filtering algorithm," *IEEE Transactions on Signal Processing*, vol. 58, pp. 4182–4194, Aug 2010.
- [21] M. Wicks, M. Rangaswamy, R. Adve, and T. Hale, "Space-time adaptive processing: a knowledge-based perspective for airborne radar," *IEEE Signal Processing Magazine*, vol. 23, no. 1, pp. 51–65, 2006.
- [22] J. Ward, "Space-time adaptive processing with sparse antenna arrays," in *the Thirty-Second Asilomar Conference on Signals, Systems & Computers, 1998*, vol. 2, pp. 1537–1541 vol.2, 1998.
- [23] Y. Wu, J. Tang, and Y. Peng, "On the essence of knowledge-aided clutter covariance estimate and its convergence," *IEEE Transactions on Aerospace and Electronic Systems*, vol. 47, no. 1, pp. 569–585, 2011.
- [24] X. Wang, E. Aboutanios, M. Trinkle, and M. Amin, "Reconfigurable adaptive array beamforming by antenna selection," *IEEE Transactions on Signal Processing*, vol. 62, pp. 2385–2396, May 2014.
- [25] E. Baranoski, "Sparse network array processing," in *Seventh IEEE Workshop on Statistical Signal and Array Processing*, pp. 145–148, 1994.
- [26] E. Aboutanios and B. Mulgrew, "Hybrid detection approach for STAP in heterogeneous clutter," *IEEE Transactions on Aerospace and Electronic Systems*, vol. 46, no. 3, pp. 1021–1033, 2010.
- [27] W. Melvin, "A STAP overview," *IEEE Aerospace and Electronic Systems Magazine*, vol. 19, no. 1, pp. 19–35, 2004.